Available online at www.sciencedirect.com
ScienceDirect
International Journal of Thermal Sciences 46 (2007) 531–539
International Journal of Thermal Sciences
www.elsevier.com/locate/ijts

# Conjugate natural convection in a porous enclosure: effect of conduction in one of the vertical walls

Nawaf H. Saeid *

*School of Mechanical Engineering, The University of Nottingham Malaysia Campus, 43500 Semenyih, Selangor, Malaysia*

Received 9 April 2006; received in revised form 8 August 2006; accepted 10 August 2006

Available online 11 September 2006

**Abstract**

Steady conjugate natural convection–conduction heat transfer in a two-dimensional porous enclosure with finite wall thickness is studied numerically in the present article. The horizontal heating is considered, where the vertical boundaries are isothermal at different temperatures with adiabatic horizontal boundaries. The Darcy model is used in the mathematical formulation for the porous layer and finite volume method is used to solve the dimensionless governing equations. The governing parameters considered are the Rayleigh number ($10 \leqslant Ra \leqslant 1000$), the wall to porous thermal conductivity ratio ($0.1 \leqslant K_r \leqslant 10$) and the ratio of wall thickness to its height ($0.02 \leqslant D \leqslant 0.5$). The results are presented to show the effect of these parameters on the heat transfer and fluid flow characteristics. The results including the streamlines and isotherm patterns and the local and average Nusselt number for different values of the governing parameters. It is found, in most of the cases that either increasing the Rayleigh number and the thermal conductivity ratio or decreasing the thickness of the bounded wall can increase the average Nusselt number for the porous enclosure ($\overline{Nu}_p$). In special cases at low $Ra$ and high conductive walls, the values of $\overline{Nu}_p$ are increasing with the increase of the wall thickness.


*Keywords:* Conjugate heat transfer; Natural convection; Porous media; Numerical study

## 1. Introduction

During the past few decades the heat transfer in the systems including fluid-saturated porous media has received considerable attention due to the wide range of geophysical and engineering applications. These include high performance insulation for buildings, grain storage, energy efficient drying processes, spreading of pollutants, etc. Representative reviews of these applications and others convective heat transfer applications in porous media may be found in the recent books by Vafai [1], Ingham and Pop [2], Pop and Ingham [3], Nield and Bejan [4] and Kaviany [5].

The natural convection in porous media has been studied extensively using different models; see, for example, [6–13]. However, the effect of the solid walls bounded the porous media is received relatively less attention. The conjugate natural convection–conduction heat transfer through solid–porous layer can be found in many engineering applications. Kimura et al. [14] presented a review of conduction–convection conjugated natural convection from plates or bodies in a fluid-saturated porous medium. Several different configurations including slender bodies, rectangular slabs, horizontal cylinders and spheres are discussed in this review paper. Mbaye et al. [15] studied both analytically and numerically the natural convection heat transfer in an inclined porous layer boarded by a wall with finite thickness and conductivity. In this study [15] a constant heat flux is applied for heating and cooling the long sidewalls of the rectangular enclosure while the other two walls are insulated. The conjugate conduction-forced convection in a plane channel filled with a saturated porous medium is investigated analytically by Nield and Kuznetsov [16]. Their results show the effect of the finite thermal resistance due to the slabs is to reduce both the heat transfer to the porous medium and the degree of local thermal non-equilibrium. Nield and Kuznetsov [17] extended their investigation [16] for forced convection in a plane channel filled with a saturated bi-disperse

* Tel.: +60 3 89248184; fax: +60 3 89248017.
*E-mail address:* n_h_saeid@yahoo.com.

1290-0729/$ – see front matter 
doi:10.1016/j.ijthermalsci.2006.08.003

**Nomenclature**

| | | | |
|---|---|---|---|
| $d$ | wall thickness | m | |
| $D$ | dimensionless wall thickness ($d/L$) | | |
| $g$ | gravitational acceleration | $m\,s^{-2}$ | |
| $K$ | permeability of the porous medium | $m^2$ | |
| $K_r$ | thermal conductivity ratio ($K_r = k_w/k_p$) | | |
| $k_p$ | effective thermal conductivity of porous medium | $W\,m^{-1}\,K^{-1}$ | |
| $k_w$ | thermal conductivity of wall | $W\,m^{-1}\,K^{-1}$ | |
| $L$ | wall height | m | |
| $Nu$ | local Nusselt number, Eq. (10) | | |
| $\overline{Nu}$ | average Nusselt number, Eq. (10) | | |
| $q'''$ | heat flux | $W\,m^{-2}$ | |
| $Ra$ | Rayleigh number for porous medium, $Ra = g\beta K(T_h - T_c)L/\upsilon\alpha$ | | |
| $T$ | temperature | K | |
| $u, v$ | velocity components along $x$- and $y$-axes, respectively | $m\,s^{-1}$ | |
| $x, y$ | Cartesian coordinates | m | |
| $X, Y$ | non-dimensional Cartesian coordinates, Eq. (5) | | |

*Greek symbols*

| | | |
|---|---|---|
| $\alpha$ | effective thermal diffusivity | $m^2\,s^{-1}$ |
| $\beta$ | coefficient of thermal expansion | $K^{-1}$ |
| $\theta$ | non-dimensional temperature, Eq. (5) | |
| $\upsilon$ | kinematic viscosity | $m^2\,s^{-1}$ |
| $\Psi$ | non-dimensional stream function, Eq. (5) | |

*Subscripts*

| | |
|---|---|
| $c$ | cold |
| $h$ | hot |
| $w$ | wall |
| $p$ | porous |
| $wp$ | wall–porous interface |

porous medium, coupled with conduction in plane slabs bounding the channel using a two-velocity, two-temperature model. The results are presented to show the dependence of Nusselt number on Biot number associated with the boundary slabs, the inter-phase heat exchange parameter, the inter-phase thermal conductivity ratio, the inter-phase effective permeability ratio, and the macroscopic void fraction. Baytas et al. [18] considered the steady conjugate natural convection in a square cavity filled with a porous medium for numerical investigation. They presented the results for the system consists of two horizontal conductive walls of finite thickness and two vertical walls at different temperatures. Conjugate natural convection in a rectangular porous cavity surrounded by walls was examined by Chang and Lin [19]. Their results show that wall conduction effects decrease the overall heat transfer rate from the hot to cold sides of the system. Chang and Lin [20] studied also the effect of wall heat conduction on natural convection in an enclosure filled with a non-Darcian porous medium. Coasta [21] used the streamlines, the heatlines and the masslines method for visualization purposes of two-dimensional steady diffusion/convection heat and mass transfer in anisotropy media without source terms. Coasta [88] illustrated this approach through pure conduction heat transfer problems, natural convection heat transfer in a porous enclosure, and conjugate conduction–convection heat transfer. Recently Mohamad and Rees [22] considered the conjugate effects on free convection from a heated vertical plate with and without a porous medium for investigation. Their results show that the rate of heat transfer may become larger for a plate embedded in a porous medium compared with bare plate at the leading edge of the plate.

The analysis of natural convection–conduction heat transfer in a two-dimensional porous layer attached to a solid impermeable wall is of practical importance in, for example, high performance insulation for buildings and cold storage installations, etc. Motivated by the lack of such an important investigation, the present study is carried out to investigate the effect of the conductive walls on the steady heat transfer through solid–porous layer.

## 2. Governing equations

A schematic diagram of horizontal heating of a porous enclosure with finite wall thickness is shown in Fig. 1. The left vertical surface of the impermeable wall is heated to a constant temperature $T_h$, and the right surface of the porous enclosure is cooled to a constant temperature $T_c$ while the horizontal walls are adiabatic. In the porous medium, Darcy's law is assumed to hold, the Oberbeck–Boussinesq approximation is used and the fluid and the porous matrix are in local thermal equilibrium.

With these assumptions, the continuity, Darcy and energy equation for steady, two-dimensional flow in an isotropic and homogeneous porous medium are:

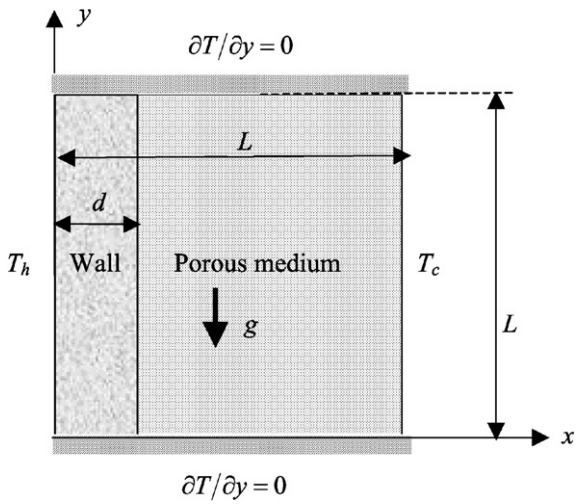


Fig. 1. Schematic diagram of the physical model and coordinate system.

$$\frac{\partial u}{\partial x}+\frac{\partial v}{\partial y}=0 \tag{1}$$

$$\frac{\partial u}{\partial y}-\frac{\partial v}{\partial x}=-\frac{g\beta K}{\upsilon}\frac{\partial T_p}{\partial x} \tag{2}$$

$$u\frac{\partial T_p}{\partial x}+v\frac{\partial T_p}{\partial y}=\alpha\left(\frac{\partial^2 T_p}{\partial x^2}+\frac{\partial^2 T_p}{\partial y^2}\right) \tag{3}$$

and the energy equation for the impermeable wall is:

$$\frac{\partial^2 T_w}{\partial x^2}+\frac{\partial^2 T_w}{\partial y^2}=0 \tag{4}$$

where the subscript $p$ for porous layer and $w$ for the wall. The above equations can be written in terms of the stream function $\psi$ defined as $u=\partial\psi/\partial y$ and $v=-\partial\psi/\partial x$ together with the following non-dimensional variables:

$$X=\frac{x}{L};\quad Y=\frac{y}{L};\quad D=\frac{d}{L}$$
$$\theta_p=\frac{T_p-T_c}{\Delta T};\quad \theta_w=\frac{T_w-T_c}{\Delta T};\quad \Psi=\frac{\psi}{\alpha} \tag{5}$$

where $\Delta T=T_h-T_c$. The resulting non-dimensional forms of the governing equations (1)–(4) are:

$$\frac{\partial^2\Psi}{\partial X^2}+\frac{\partial^2\Psi}{\partial Y^2}=-Ra\frac{\partial\theta_p}{\partial X} \tag{6}$$

$$\frac{\partial\Psi}{\partial Y}\frac{\partial\theta_p}{\partial X}-\frac{\partial\Psi}{\partial X}\frac{\partial\theta_p}{\partial Y}=\frac{\partial^2\theta_p}{\partial X^2}+\frac{\partial^2\theta_p}{\partial Y^2} \tag{7}$$

$$\frac{\partial^2\theta_w}{\partial X^2}+\frac{\partial^2\theta_w}{\partial Y^2}=0 \tag{8}$$

where $Ra$ is the Rayleigh number defined as: $Ra=g\beta K\Delta T L/\upsilon\alpha$. The values of the non-dimensional stream function are zero in the wall region and the external boundaries of the porous enclosure. The boundary conditions for the non-dimensional temperatures are:

$$\theta_w(0,Y)=1;\qquad \theta_p(1,Y)=0 \tag{9a}$$

$$\partial\theta_p(X,0)/\partial Y=0;\qquad \partial\theta_w(X,0)/\partial Y=0 \tag{9b}$$

$$\partial\theta_p(X,1)/\partial Y=0;\qquad \partial\theta_w(X,1)/\partial Y=0 \tag{9c}$$

$$\theta_p(D,Y)=\theta_w(D,Y);\quad \partial\theta_p(D,Y)/\partial X=K_r\partial\theta_w(D,Y)/\partial X \tag{9d}$$

where $K_r=k_w/k_p$ is the thermal conductivity ratio. The physical quantities of interest in this problem are the local Nusselt number and the average Nusselt number, defined respectively by:

$$Nu_w=\frac{q'''L}{k_w\Delta T}=\left(-\frac{\partial\theta_w}{\partial X}\right)_{X=0,D}$$
$$Nu_p=\frac{q'''L}{k_p\Delta T}=\left(-\frac{\partial\theta_p}{\partial X}\right)_{X=D,1} \tag{10a}$$

$$\overline{Nu}=\int_0^1 Nu\,\mathrm{d}Y \tag{10b}$$

where $q'''$ is the heat flux and $Nu_w$ is representing the dimensionless heat transfer through the walls. According to condition (9d), the following relation must be satisfied $Nu_p=K_r\times Nu_w$.

## 3. Numerical method

Eqs. (6) to (8), subjected to the boundary conditions (9), are integrated numerically using the finite volume method [23,24]. The quadratic upwind differencing QUICK scheme [25] is used for the convection–diffusion formulation in Eq. (7). This scheme uses three-point quadratic interpolation for the control volume face values of the dependent variable. Implementation of the boundary conditions for the porous layer required a separate integration for the boundary and near boundary control volumes as well as the corner control volumes. The linear extrapolation, known as mirror node approach, has been used for the boundary conditions implementation. Although a $(40\times 40)$ mesh gives acceptable results for zero wall thickness [26], $(100\times 100)$ uniform spacing mesh is used for the computational domain to ensure enough grid points in the different regions. In the solution domain, the external boundaries as well as the wall–porous interface, are laying on the control volume interface. The conditions at the interfaces (9d) have been implemented by approximating the temperature gradient in the wall region using the temperature at the interface and nearest two gird points. Similar method is used for the porous medium and the temperature gradient is approximated by three-point forward difference scheme. The resultant wall–porous interface temperature can be derived as:

$$\theta_{wp}(i,Y)=\frac{9\theta_p(i,Y)-\theta_p(i+1,Y)}{8(1+K_r)}+\frac{K_r[9\theta_w(i-1,Y)-\theta_w(i-2,Y)]}{8(1+K_r)} \tag{11}$$

The resulting algebraic equations were solved line-by-line using the Tri-Diagonal Matrix Algorithm iteration procedure. The iteration process is terminated under the following condition:

$$\sum_{i,j}\left|\phi^n_{i,j}-\phi^{n-1}_{i,j}\right|\Big/\sum_{i,j}\left|\phi^n_{i,j}\right|\leqslant 10^{-7} \tag{12}$$

where $\phi$ stands for $\theta_w,\theta_p$ and $\Psi$ and $n$ denotes the iteration step. The Nusselt number defined in Eq. (10) is calculated by using the boundary and the next two grid values of the non-dimensional temperature in the $X$-direction. This numerical method has been discussed and successfully used in the study of the natural convection in porous cavity by Saeid and Mohamad [26]. The average Nusselt number is calculated from the local values along $X=0$ and $X=D$ for the wall side and along $X=D$ and $X=1$ for the porous side. The results show satisfaction of both the energy equations, where the values of $\overline{Nu}_w$ are equal at $X=0$ and $X=D$ and the values of $\overline{Nu}_p$ are equal at $X=D$ and $X=1$.

## 4. Results and discussion

The results are generated for different values of the governing parameters, which are the Rayleigh number ($10\leqslant Ra\leqslant 1000$), thermal conductivity ratio ($0.1\leqslant K_r\leqslant 10$) and the ratio of wall thickness to its height ($0.02\leqslant D\leqslant 0.5$).

To show the effect of the wall thickness $D$ on the thermal fields and the circulation of the fluid in the porous enclosure, the

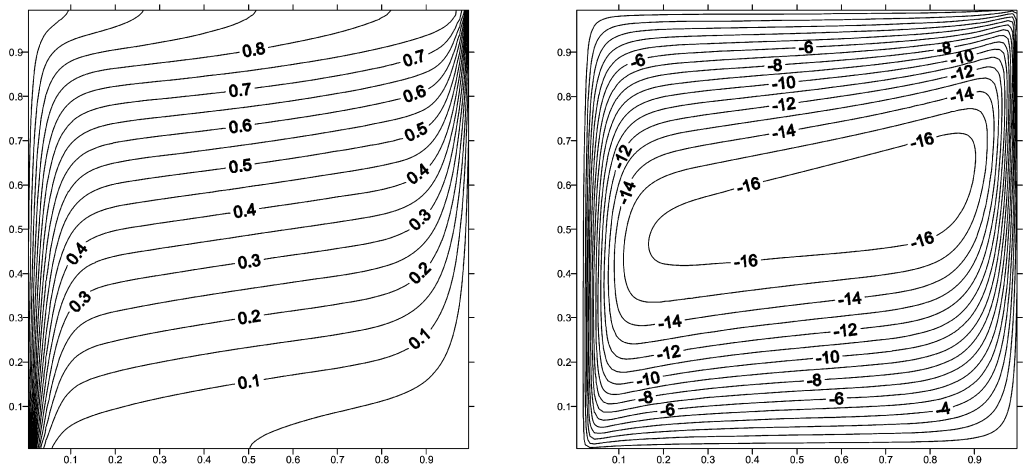

(a) $D = 0.02$, $\overline{Nu}_p = 10.041$, $\overline{Nu}_w = 10.041$

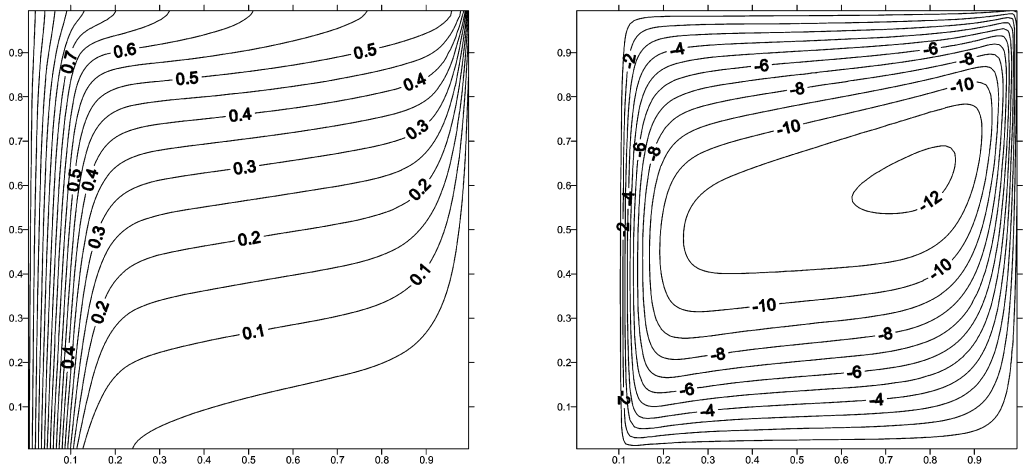

(b) $D = 0.10$, $\overline{Nu}_p = 5.044$, $\overline{Nu}_w = 5.044$

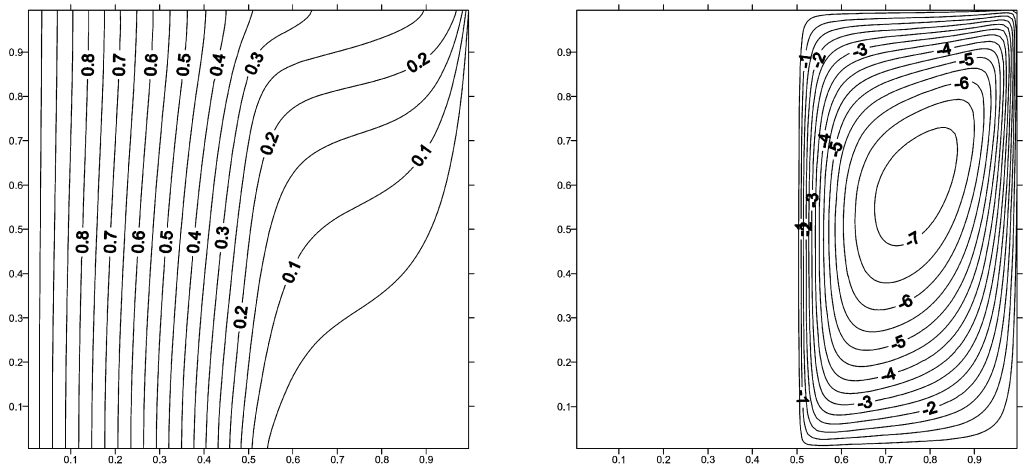

(c) $D = 0.50$, $\overline{Nu}_p = 1.566$, $\overline{Nu}_w = 1.566$

Fig. 2. Isotherms (left), streamlines (right) at $Ra = 1000$ and $K_r = 1.0$.

isotherms and streamlines are presented in Fig. 2 for $Ra = 1000$ and $K_r = 1$. As the wall thickness increases the average Nusselt numbers decreases, which indicates conduction domination heat transfer in the system. The strength of the circulation of the fluid saturated the porous medium is much higher with thin walls. It is important to note that the Rayleigh number in the present study is based on the wall height and not on the thickness of the porous layer.

The variation of wall–porous interface temperature is shown in Fig. 3 for different values of wall thickness $D$ and con-

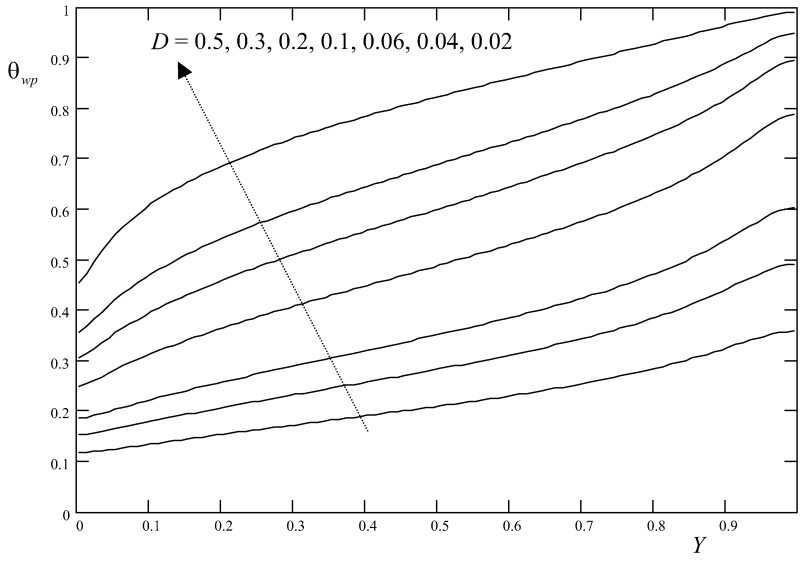


Fig. 3. Variation of wall–porous interface temperature at constant $K_r = 1$ and $Ra = 1000$.

stant $K_r = 1$ and $Ra = 1000$. The natural convection inside the porous enclosure is driven by the temperature difference between the interface and the cold boundary. It is observed that this temperature difference is reducing with increasing the wall thickness as shown in Fig. 3 and therefore reducing the average Nusselt number.

The isotherms and streamlines are shown in Fig. 4 for different values of the thermal conductivity ratio parameter and constant $Ra = 1000$ and $D = 0.2$. It can be seen from Fig. 4 that, the strength of the fluid circulation in the porous medium is increasing with the increase of the thermal conductivity ratio. This is due to the thermal field in the porous layer, where the temperature gradient in the horizontal direction is increasing with the increase in $K_r$ (i.e. good conductive wall).

Fig. 5 shows the variation of wall–porous interface temperature for different values of the thermal conductivity ratio and at constant $D = 0.2$ and $Ra = 1000$. For high values of $K_r$ (conductive wall) the temperature difference between the interface and the cold boundary is high as shown in Fig. 5. In contrast to that for walls with poor thermal conductivity, the temperature difference between the interface and the cold boundary is small and lead to reduce the average Nusselt number.

The calculated average Nusselt number for both wall and porous layer are given in Figs. 2 and 4. These results presented in Figs. 2 and 4 show the correct implementation of the boundary condition at the wall–porous layer interface, where $\overline{Nu}_p = K_r \times \overline{Nu}_w$.

The variations of the local Nusselt number along the wall–porous layer interface ($X = D$) are shown in Fig. 6 for constant $Ra = 1000$ and $D = 0.2$. The values of local Nusselt number along the outer surface of the wall ($X = 0$) are calculated also and the results are presented as $K_r \times Nu_w$ in Fig. 6 for comparison. Fig. 6 shows the usual decrease of both $Nu_p$ and $K_r \times Nu_w$ at the upper part of the wall since this region has relatively high temperature. It is worth mentioning that for low values of $K_r$, where the solid wall is insulation material, the variation of the local Nusselt number have low values compare with those at high values of $K_r$. This is a logical result since reducing the thermal conductivity of the wall leads to the increase in the thermal resistance of the overall system and therefore reducing the Nusselt number.

The resultant variation of the average Nusselt number with the Rayleigh number is shown in Fig. 7 for different values of $D$ and $K_r = 0.1$, 1.0 and 10.0. Fig. 7 shows that reducing the solid wall thickness leads to the enhancement in the heat transfer by natural convection and increase the average Nusselt number for $K_r = 0.1$ and 1.0. The unusual behavior of the highly conductive walls ($K_r = 10$) is observed at low values of $Ra$ ($Ra < 100$) where it is found that $\overline{Nu}_p$ is reducing with reducing the wall thickness. This means that the thermal resistance of the wall is less than that of the porous medium for highly conductive walls and $Ra < 100$.

To show this unusual behavior, the variation of $\overline{Nu}_p$ with the wall thickness $D$ is plotted in Fig. 8 at different values of $K_r$ with $Ra = 10$ and $Ra = 50$. Fig. 8 shows that at $Ra = 10$ and high conductive walls ($K_r = 2$ and $K_r = 10$) the values of $\overline{Nu}_p$ are increasing with the increase of the wall thickness. In contrast to that the values of $\overline{Nu}_p$ are decreasing sharply with the increase of the wall thickness with low thermal conductivity (e.g., $K_r = 0.1$) as shown in Fig. 8. The results with $Ra = 50$ show similar variation of $\overline{Nu}_p$ with $D$ but the wall should be with higher thermal conductivity ($K_r = 10$) in order to get $\overline{Nu}_p$ increasing with the increase in $D$ as shown in Fig. 8. The calculated values of $\overline{Nu}_p$ for low values of $K_r$ (e.g., $K_r = 0.1$ to 0.5) and thick walls show approximately constant at different low values of $Ra$ as shown in Figs. 7 and 8. It is found that $\overline{Nu}_p \approx 3.1$ at $Ra = 100$ and $K_r = 10$ for all the values of $D$ ($0.02 \leqslant D \leqslant 0.5$), which means that there is no effect of the wall thickness on the values of $\overline{Nu}_p$ as shown in Fig. 7. For $Ra > 100$ and $K_r = 10$ the values of $\overline{Nu}_p$ start to increase with the decrease of the wall thickness. Fig. 7 also shows that the increase of $\overline{Nu}_p$ with decreasing

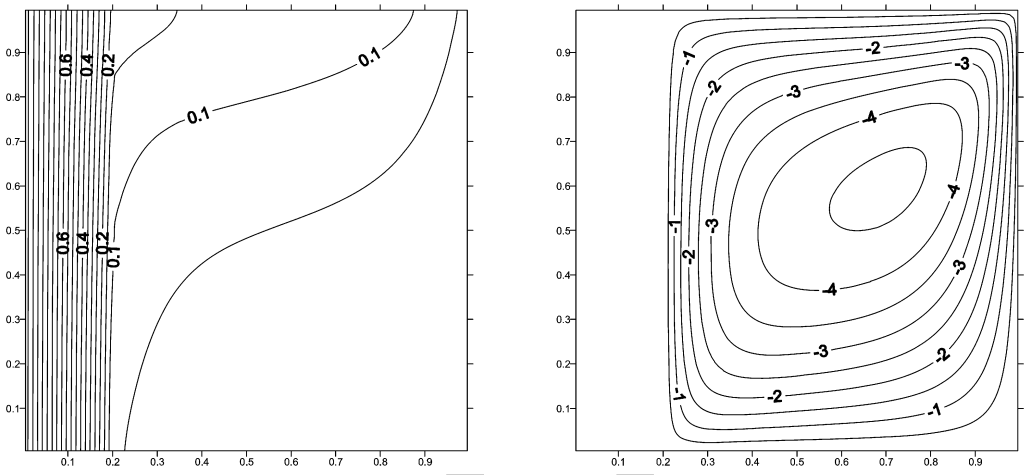

(a) $K_r = 0.1$, $\overline{Nu}_p = 0.446$, $\overline{Nu}_w = 4.460$

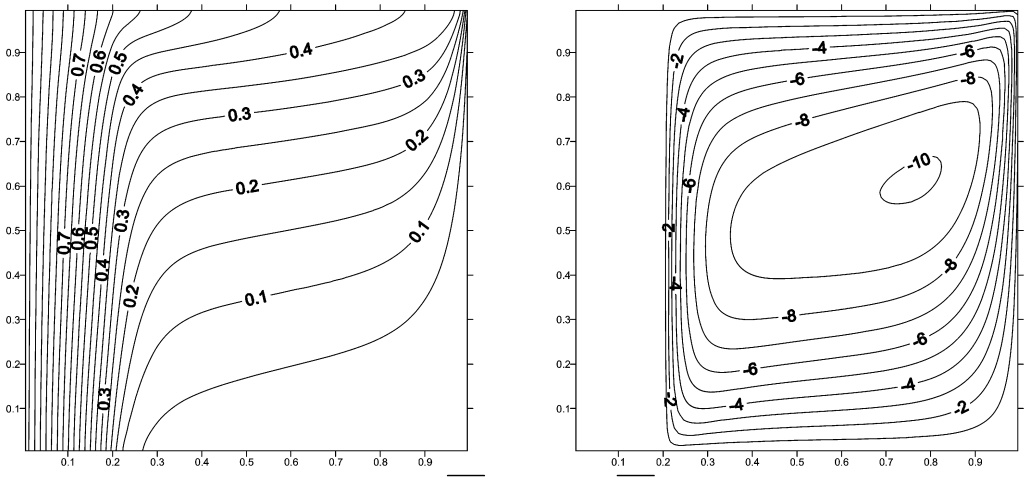

(b) $K_r = 1.0$, $\overline{Nu}_p = 3.186$, $\overline{Nu}_w = 3.186$

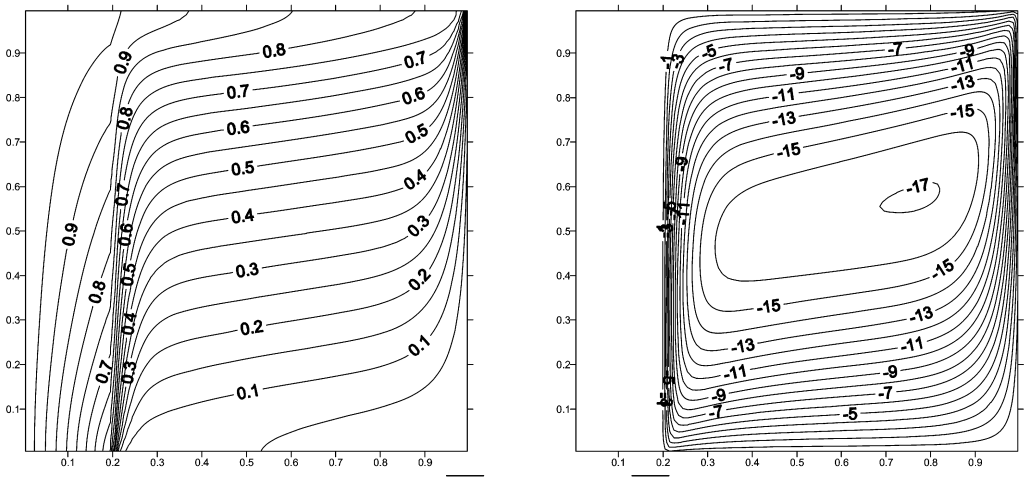

(c) $K_r = 10.0$, $\overline{Nu}_p = 10.235$, $\overline{Nu}_w = 1.024$

Fig. 4. Isotherms (left), streamlines (right) at $Ra = 1000$ and $D = 0.2$.

the wall thickness is more with low values of $K_r$ than those with high values of $K_r$. For small values of Rayleigh number, where the heat is transferred mainly by conduction in both wall and porous layer, the average Nusselt number is approximately constant as shown in Fig. 7. The results presented in Fig. 7 show that as *Ra* increases the average Nusselt number is increasing with higher slop for the thin walls than that for thick walls.

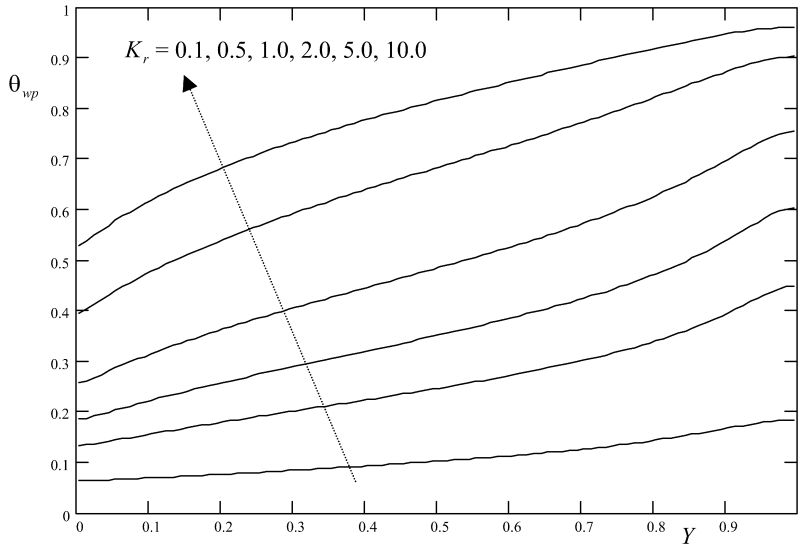


Fig. 5. Variation of wall–porous interface temperature at constant $D = 0.2$ and $Ra = 1000$.

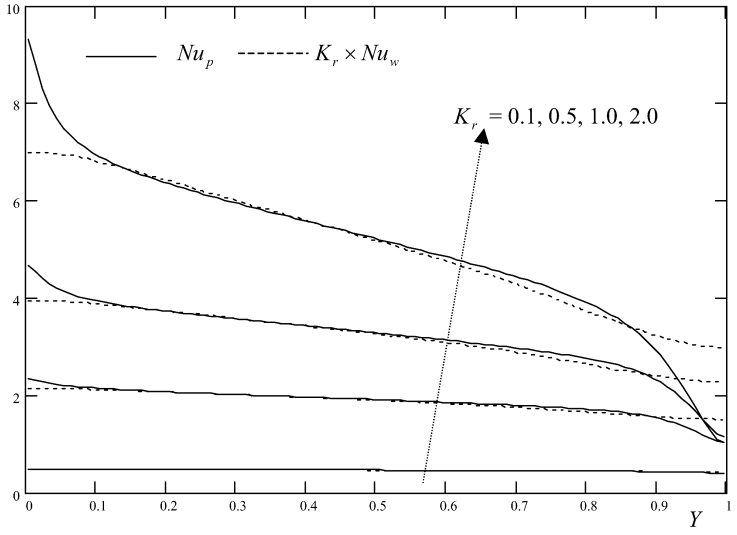


Fig. 6. Local Nusselt number along hot and cold walls at $Ra = 1000$ and $D = 0.2$.

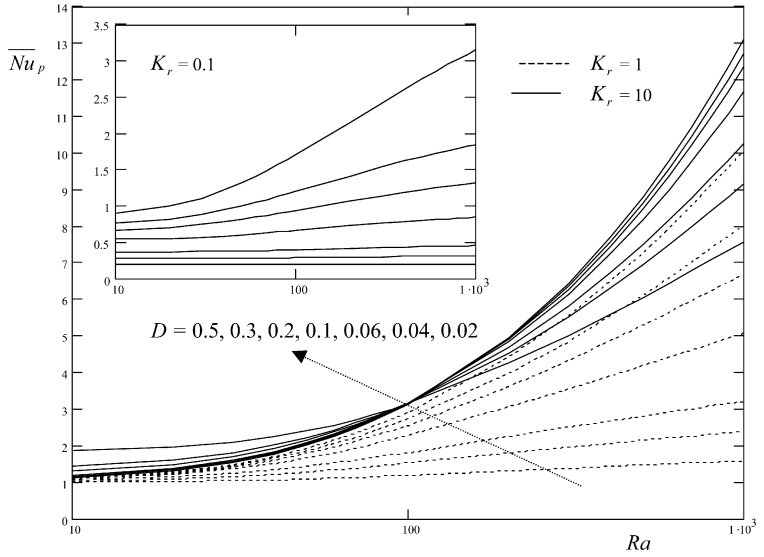


Fig. 7. Variation of $\overline{Nu}_p$ with $Ra$.

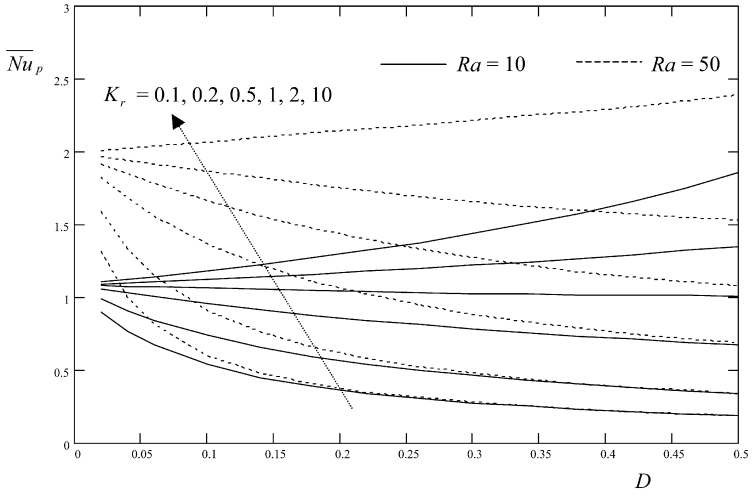


Fig. 8. Variation of $\overline{Nu}_p$ with $D$.

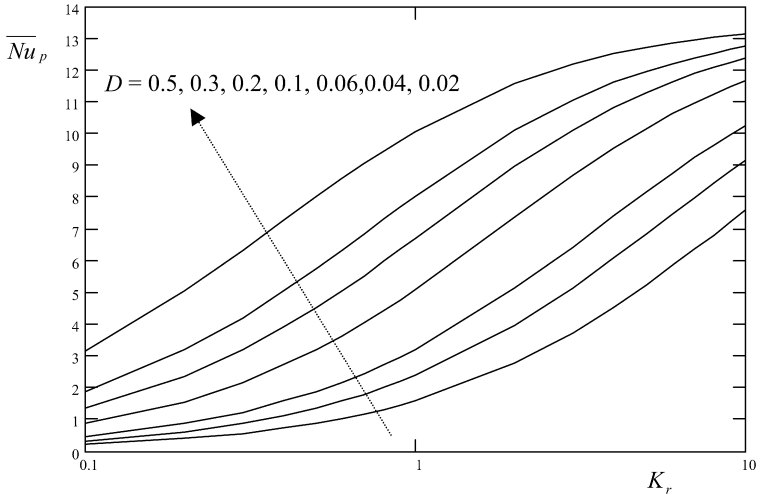


Fig. 9. Variation of $\overline{Nu}_p$ with $K_r$ at $Ra = 1000$.

Finally the effect of both the wall thickness and the thermal conductivity ratio on the heat transfer is studied with constant $Ra = 1000$ and the results are depicted in Fig. 9.

As indicated earlier the local and therefore the average Nusselt number are increasing with the increase of the thermal conductivity ratio parameter as shown in Fig. 9. The increase in $\overline{Nu}_p$ with $K_r$ for thin walls (small $D$) is sharper at low values of $K_r$ ($K_r < 1$) than that at high values of $K_r$. In contrast to that, the increase in $\overline{Nu}_p$ with $K_r$ for thick walls ($D > 0.1$), where $\overline{Nu}_p$ is approximately constant at ($K_r < 1$). The results presented in Fig. 9 shows the variation of $\overline{Nu}_p$ is increasing with the increase in $K_r$ sharply at ($K_r > 1$) for thick walls ($D > 0.1$). This indicates the effect of the conduction heat transfer on the natural convection through the porous enclosure. It can be predicted from Fig. 9 that as $D \to 0$ and high values of $K_r$ the average Nusselt number will approximate the respective value of the ideal cavity with isothermal vertical boundaries ($\overline{Nu}_p \approx 13.50$ at $Ra = 1000$).

The values of the dimensionless heat transfer $\overline{Nu}_w$ can be calculated from the results presented in Figs. 7 to 9 using $\overline{Nu}_w = \overline{Nu}_p / K_r$.

## 5. Conclusions

Numerical investigation is carried out for the steady conjugate natural convection–conduction heat transfer in a two-dimensional vertical porous enclosure with finite wall thickness. The vertical boundaries are isothermal at different temperatures with adiabatic horizontal walls. The governing parameters are the ratio of the wall thickness to its height ($D$), the wall to porous thermal conductivity ratio ($K_r$) and the Rayleigh number ($Ra$). The results are presented to show the effect of these parameters on the heat transfer and fluid flow characteristics. It is observed that the temperature difference between the interface and the cold boundary is reducing with increasing the wall thickness and therefore reducing the average Nusselt num-

ber. It is found that as the wall thickness increases the average Nusselt numbers decreases, and the strength of the circulation of the fluid saturated the porous medium is much higher with thin walls. It is found for special cases at low $Ra$ ($Ra = 10$) and high conductive walls ($K_r = 10$), the values of $\overline{Nu}_p$ are increasing with the increase of the wall thickness. For low values of $K_r$, where the solid wall is insulation material, the variations of the local Nusselt number have low values compare with those at high values of $K_r$ because of the increase in the thermal resistance of the overall system and visa versa. The numerical results indicated that for small values of Rayleigh number, where the heat is transferred mainly by conduction in both wall and porous layer, the average Nusselt number is approximately constant. As $Ra$ increases the average Nusselt number is increasing with higher slop for the thin walls than that for thick walls.

## References


[1] K. Vafai (Ed.), Handbook of Porous Media, second ed., Taylor & Francis, New York, 2005.

[2] D.B. Ingham, I. Pop (Eds.), Transport Phenomena in Porous Media, vol. III, Elsevier, Oxford, 2005.

[3] I. Pop, D.B. Ingham, Convective Heat Transfer: Mathematical and Computational Modelling of Viscous Fluids and Porous Media, Pergamon, Oxford, 2001.

[4] D.A. Nield, A. Bejan, Convection in Porous Media, third ed., Springer, New York, 2006.

[5] M. Kaviany, Principles of Heat Transfer in Porous Media, second ed., Springer, New York, 1995.

[6] P.J. Burns, L.C. Chow, C.L. Tien, Convection in a vertical slot filled with porous insulation, Int. J. Heat Mass Transfer 20 (1977) 919–926.

[7] V. Prasad, F.A. Kulacki, Natural convection in a rectangular cavity with constant heat flux on one vertical wall, ASME J. Heat Transfer 106 (1984) 152–157.

[8] F.C. Lai, F.A. Kulacki, Natural convection across a vertical layered porous cavity, Int. J. Heat Mass Transfer 31 (1988) 1247–1260.

[9] Y.F. Rao, E.K. Glakpe, Natural convection in a vertical slot filled with porous medium, Int. J. Heat Fluid Flow 13 (1992) 97–99.

[10] A.A. Mohamad, Non-equilibrium, natural convection in a differentially heated cavity filled with a saturated porous matrix, ASME J. Heat Transfer 122 (2000) 380–384.

[11] N.H. Saeid, Analysis of mixed convection in a vertical porous layer using non-equilibrium model, Int. J. Heat Mass Transfer 47 (2004) 5619–5627.

[12] N.H. Saeid, I. Pop, Natural convection from discrete heater in a square cavity filled with a porous medium, J. Porous Media 8 (2005) 55–63.

[13] N.H. Saeid, I. Pop, Non-Darcy natural convection in a square cavity filled with a porous medium, Fluid Dynamics Research 36 (2005) 35–43.

[14] S. Kimura, T. Kiwata, A. Okajima, I. Pop, Conjugate natural convection in porous media, Advances in Water Resources 20 (1997) 111–126.

[15] M. Mbaye, E. Bilgen, P. Vasseur, Natural-convection heat transfer in an inclined porous layer boarded by a finite-thickness wall, Int. J. Heat Fluid Flow 14 (1993) 284–291.

[16] D.A. Nield, A.V. Kuznetsov, Local thermal nonequilibrium effects in forced convection in a porous medium channel: a conjugate problem, Int. J. Heat Mass Transfer 42 (1999) 3245–3252.

[17] D.A. Nield, A.V. Kuznetsov, Forced convection in a bi-disperse porous medium channel: a conjugate problem, Int. J. Heat Mass Transfer 47 (2004) 5375–5380.

[18] A.C. Baytas, A. Liaqat, T. Grosan, I. Pop, Conjugate natural convection in a square porous cavity, Heat Mass Transfer 37 (2001) 467–473.

[19] W.J. Chang, H.C. Lin, Natural convection in a finite wall rectangular cavity filled with an anisotropic porous medium, Int. J. Heat Mass Transfer 37 (1994) 303–312.

[20] W.J. Chang, H.C. Lin, Wall heat conduction effect on natural convection in an enclosure filled with a non-Darcian porous medium, Numerical Heat Transfer, Part A 25 (1994) 671–684.

[21] V.A.F. Costa, Unified streamline, heatline and massline methods for the visualization of two-dimensional heat and mass transfer in anisotropic media, Int. J. Heat Mass Transfer 46 (2003) 1309–1320.

[22] A.A. Mohamad, D.A.S. Rees, Conjugate free convection in a porous medium attached to a wall held at a constant temperature, in: A.H. Reis, A.F. Miguel (Eds.), Applications of Porous Media (ICAPM 2004), Évora, Portugal, pp. 93–97.

[23] S.V. Patankar, Numerical Heat Transfer and Fluid Flow, in: W.J. Minkowycz, E.M. Sparrow (Eds.), Computational Methods in Mechanics and Thermal Sciences, McGraw-Hill, New York, 1980.

[24] H.K. Versteeg, W. Malalasekera, An Introduction to Computational Fluid Dynamics, the Finite Volume Method, Longman, England, 1995.

[25] T. Hayase, J.A.C. Humphrey, R. Greif, A consistently formulated QUICK scheme for fast and stable convergence using finite-volume iterative calculation procedures, J. Comput. Phys. 98 (1992) 108–118.

[26] N.H. Saeid, A.A. Mohamad, Natural convection in a porous cavity with spatial sidewall temperature variation, Int. J. of Numerical Methods for Heat & Fluid Flow 15 (2005) 555–566.